Structural studies on cationic poly{9,9-*bis*[6-(*N*,*N*,*N*-trimethylammonium)alkyl]fluorene-*co*-1,4-phenylene} iodides in aqueous solutions in the presence of the non-ionic surfactant pentaethyleneglycol monododecyl ether ($C_{12}E_5$)

2008 J. Phys.: Condens. Matter 20 104210

(http://iopscience.iop.org/0953-8984/20/10/104210)

J. Phys.: Condens. Matter **20** (2008) 104210 (7pp) doi:10.1088/0953-8984/20/10/104210

Structural studies on cationic poly{9,9-*bis*[6-(*N*,*N*,*N*-trimethylammonium)alkyl]fluorene-*co*-1,4-phenylene} iodides in aqueous solutions in the presence of the non-ionic surfactant pentaethyleneglycol monododecyl ether ($C_{12}E_5$)

H D Burrows[1], M Knaapila[2,6], A P Monkman[2], M J Tapia[3], S M Fonseca[1], M L Ramos[1], W Pyckhout-Hintzen[4], S Pradhan[5,7] and U Scherf[5]

[1] Departamento de Química, Universidade de Coimbra, 3004-535 Coimbra, Portugal
[2] OEM Research Group, Department of Physics, University of Durham, Durham DH1 3LE, UK
[3] Departamento de Química, Universidad de Burgos, Burgos 09001, Spain
[4] Institut für Festkörperforschung, FZ Jülich, 52425, Jülich, Germany
[5] Makromolekulare Chemie, Bergische Universität Wuppertal, D-42097, Germany

E-mail: burrows@ci.uc.pt

Received 15 July 2007, in final form 28 September 2007
Published 19 February 2008
Online at stacks.iop.org/JPhysCM/20/104210

Abstract

Two cationic conjugated polyelectrolyte poly{9,9-*bis*[6-(*N*,*N*,*N*-trimethylammonium)alkyl]fluorene-*co*-1,4-phenylene} iodides in aqueous solution in the presence of the non-ionic surfactant pentaethyleneglycol monododecyl ether ($C_{12}E_5$) were studied using optical absorption and fluorescence, NMR, and small-angle neutron scattering (SANS) with a model of randomly arranged core–shell cylinders in a solvent. The polymers differed in both the size of the aromatic backbone and the length of the alkyl side chains. In agreement with studies on related conjugated polyelectrolytes, optical observations indicate that the surfactant breaks up clusters of the polymer and produces solutions of mixed polyelectrolyte–surfactant aggregates. The SANS data are in accord with the idea of dissolution and show that with $C_{12}E_5$ surfactant these polymers form long worm-like particles which contain rigid segments with the diameter of 5 nm. With the ternary system involving the polymer with a larger backbone, longer rigid segments were observed, for which a typical value of >60 nm was calculated. In contrast, for the smaller polymer the value is around 45 nm. This difference is rationalized on the basis of the difference in polymer size.

(Some figures in this article are in colour only in the electronic version)

[6] Present address: MAX-lab, Lund University, PO Box 118, SE-221 00 Lund, Sweden.
[7] Present address: Max Planck Institute for Polymer Research, Ackermannweg 10, 55128 Mainz, Germany.

1. Introduction

Conjugated polyelectrolytes are important materials, with applications in areas such as chemical/biological sensors [1–15], charge injection and transport layers [16–20], and have potential in areas such as photovoltaic systems and light emitting diodes (LEDs). These ionic conjugated polymers are also relevant for applications in self-assembly [21, 22] and for film preparation using solvent based methodologies, such as inkjet and screen printing [23, 24]. Fluorene based polymers show particular potential for these applications because of their blue emission and high luminescence yields, and, in addition, have a rigid-rod structure, which means that there is a possibility of forming nematic liquid crystal phases [25]. However, conjugated polyelectrolytes containing the fluorene moiety tend to aggregate in aqueous solutions, leading to inter-chain interactions which greatly reduce luminescence yields [26]. Both organic cosolvents [5, 20] and surfactants [12, 15, 27–31] have been used to break up these polymer aggregates. We have shown with the anionic conjugated polyelectrolyte poly{1,4-phenylene-[9,9-*bis*(4-phenoxybutylsulfonate)]fluorene-2,7-diyl} (PBS-PFP) that this can be achieved by addition of the non-ionic surfactant pentaethyleneglycol monododecyl ether ($C_{12}E_5$) [27, 28]. Small-angle neutron scattering (SANS) experiments [29] have suggested that this is due to formation of mixed surfactant–polyelectrolyte aggregates and these results and dynamic light scattering measurements (unpublished data) suggest that at high surfactant concentrations these may have elongated, worm-like structures. These may be similar to the fibre-like aggregates seen in cryogenic transmission electron microscopy with poly(paraphenylene) amphiphilic polymers in aqueous solutions in the presence of non-ionic alkyl oxyethylene surfactants [32]. Such aggregates are of interest within the general context of polyfluorene based nanoscale assemblies [33].

Particular interest is currently being focused on the use of cationic fluorene based conjugated polyelectrolytes as conjugates for DNA studies [3, 5–8, 15]. We have therefore extended our structural studies on fluorene based conjugated polyelectrolytes in aqueous solutions in the presence of the surfactant $C_{12}E_5$ to two cationic poly{9,9-*bis*[6-(*N*,*N*,*N*-trimethylammonium)alkyl]fluorene-*co*-1,4-phenylene} iodides, PFP-NR3, having six methylene groups between the aromatic backbone and the alkylammonium group, and a commercial analogue, ADS 181, in which there are three methylene groups in each alkyl chain. The structures are given in figure 1. These have been studied using SANS, ^{1}H NMR spectroscopy and photophysical measurements.

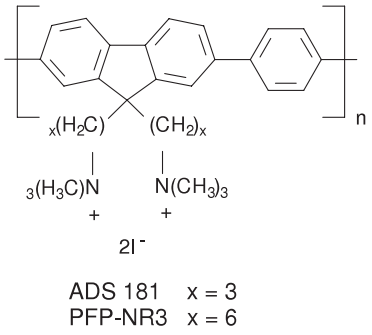

Figure 1. Structures of the polymers studied.

2. Experimental procedures

The synthesis of PFP-NR3, poly{9,9-*bis*[6-(*N*,*N*,*N*-trimethylammonium)alkyl]fluorene-*co*-1,4-phenylene} iodide, has been described in detail elsewhere [34]. This has a molecular weight (M_n) determined by gel permeation chromatography on a precursor of 3500, which corresponds to 4–5 repeat units. The conjugated polyelectrolyte ADS 181 (M_n 10 000, corresponding to about 15 repeat units) was obtained from American Dye Sources (Quebec, Canada). This was stored in the absence of light as it was found to photodegrade in solution. Although it is thought that the length of the alkyl side chains does not significantly affect the aggregation behaviour, future studies are planned in which cationic conjugated polyelectrolytes having the same sized alkyl chains but different numbers of repeat units will be studied. Pure *n*-dodecylpentaoxyethylene glycol ether ($C_{12}E_5$) was a gift from Professor Ulf Olsson (Lund University) and was used without further treatment. Experiments were also carried out with commercial $C_{12}E_5$ (Fluka) and gave similar results. Ternary polymer–surfactant–water solutions were prepared with D_2O (>99%, GOSS Scientific Instruments Ltd) to form the D_2O–polymer–$(C_{12}E_5)_x$ system at the appropriate molar ratio x with respect to the polymer repeat unit. Samples were stirred for 1 day and, when necessary, ultrasound agitation used to ensure uniformity. Samples were measured within 1 day of preparation. Absorption and fluorescence spectra were recorded on Shimadzu UV-2100 and Horiba–Jobin–Ivon SPEX Fluorog 3–22 spectrometers, respectively. The fluorescence spectra were corrected for the wavelength response of the system. The fluorescence quantum yields were measured using tetrathiophene ($\phi_F = 0.33$ in MCH [35]) and quinine sulfate [36] as standards as described elsewhere [36]. ^{1}H NMR spectra were obtained on a Varian UNITY-500 NMR spectrometer. The same solutions were used as in the SANS measurements.

SANS experiments were performed at the KWS1 spectrometer at the FRJ-2 Reactor, Research Centre Jülich, Germany. Data were collected at sample-to-detector distances of 2, 8 and 20 m, leading to a scattering vector range q between 0.002 and 0.2 Å^{-1} approximately using a neutron wavelength $\lambda = 7$ Å. The wavelength spread $\Delta\lambda/\lambda$ was 0.20. These distances provide the full scattering angle range and overlap nicely, which avoids systematic errors due to different counting statistics. The incoming neutron beam with entrance 30×30 mm^2 was collimated with respectively 4, 8 and 20 m to a sample aperture of 10×10 mm^2 to achieve maximum possible flux at the sample. The magnitude of the scattering vector q is related to the scattering angle (2θ) via $q = 4\pi/\lambda \cdot \sin(2\theta/2)$. The resolution of the detector was 128×128 channels each of 5.2 mm $\times$ 5.2 mm. Its dead time τ is 4.5 μs, allowing integral counting rates of approximately 20 000 counts per second and taken into account during normalization. Transmissions were

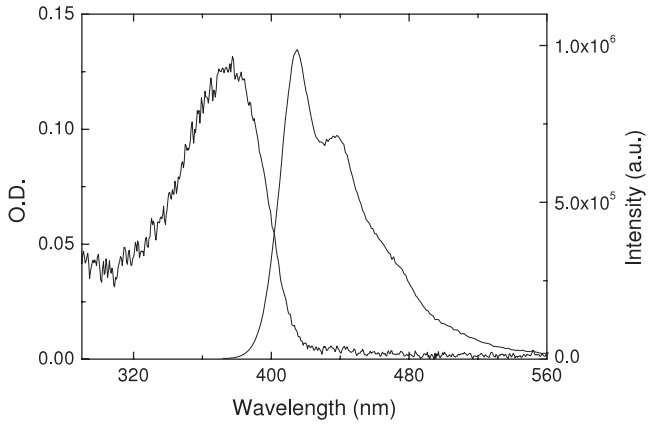

Figure 2. Absorption and fluorescence spectra of PFP-NR3 (4.96×10^{-6} M in terms of repeat units) in an aqueous solution of $C_{12}E_5$ (8×10^{-5} M).

measured *in situ* from a monitor at $q = 0$ located inside the beamstop.

The sensitivity of the detector channels was obtained from the measurement of a flat-scattering incoherent sample, i.e. Plexiglas, and every cell was corrected for it pixelwise. The corrected intensities are obtained after appropriate subtraction of empty cell scattering, background noise due to stray neutrons and γ photons, and dark current noise from the electronics. Absolute cross-sections (here further abbreviated as intensities I) were obtained after calibrating with a 1.5 mm thick secondary standard of Plexiglas, previously calibrated to vanadium and obtained as

$$\frac{\mathrm{d}\Sigma}{\mathrm{d}\Omega}(q) = \frac{\left(T_\mathrm{p} D_\mathrm{p} \frac{\mathrm{d}\Sigma_\mathrm{p}}{\mathrm{d}\Omega}\right) L_\mathrm{S}^2}{T_\mathrm{S} T_\mathrm{EC} D_\mathrm{S} L_\mathrm{p}^2 \langle I_\mathrm{p} \rangle} [(I_\mathrm{S} - I_\mathrm{BC}) - T_\mathrm{S}(I_\mathrm{EC} - I_\mathrm{BC})] \varepsilon_{ij}, \quad (1)$$

where subscripts p, S, EC, and BC stand for Plexiglas, sample, empty cell and boron carbide, respectively. The detector sensitivity correction is contained in the ε_{ij} matrix. The thickness of each component in the beam is stored in D and T denotes the transmission of the respective component to air. The detector distance is symbolized by L and defines the solid angle as $\mathrm{d}\Omega = (\text{pixel area})/L^2$. All above corrections are performed in 2D (128×128) pixelwise after which a radial averaging of the data—i.e. gathering of intensities at the same scattering vector—reduces the full 2D data to I versus q data. The absolute intensity scale (cm^{-1}) allows comparison and distinction between theoretical model functions. All solutions were contained in Hellma quartz cells of path lengths of 1 or 2 mm. The transmissions were measured *in situ* from a monitor at $q = 0$ inside the beamstop. All measurements were made using a Julabo thermostat kept at 20 °C.

3. Results and discussion

The two conjugated polyelectrolytes PFP-NR3 and ADS 181 showed low solubility in water, but dissolved readily in aqueous solutions of $C_{12}E_5$ at concentrations above the critical micelle concentration (cmc $\approx$ 50 μM [37]). The absorption and fluorescence spectra are shown in figure 2, and strongly suggest that the polymer is present as an isolated chain. The moderately high fluorescence quantum yield observed, $\Phi_\mathrm{f} = 0.27 \pm 0.02$, in these systems using tetrathiophene and quinine sulfate as standards is in agreement with this.

More details of the photophysics of PFP-NR3 in this system are reported elsewhere [15]. Proton NMR spectra were recorded in D_2O solutions of solutions of $C_{12}E_5$ alone (10 mM) and in the presence of various concentrations of ADS 181, and data are given in figure 3. Assignment of the peaks was based

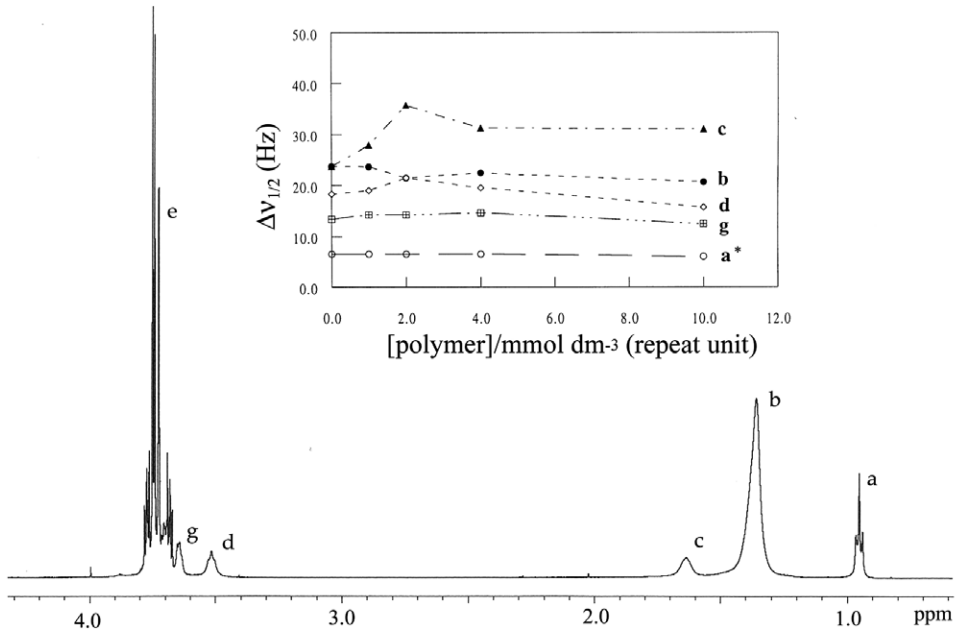

Figure 3. ^{1}H NMR spectrum with linewidths (inset) observed in D_2O solutions of $C_{12}E_5$ alone (10 mM) and in the presence of various concentrations of ADS 181. Note that for the CH_3 protons the coupling constant $J_{CH_3-CH_2}$ is used instead of the linewidth.

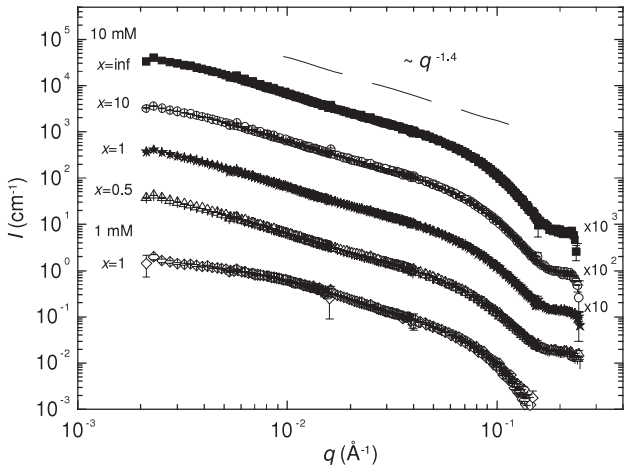

Figure 4. The SANS data for ADS 181$(C_{12}E_5)_x$ for $x = 0.5$ (triangles), $x = 1$ (stars), and $x = 10$ (open circles), where x is the molar ratio of surfactant molecules per monomer unit. The surfactant concentration was 10 mM. The data for the corresponding pure aqueous surfactant are shown by solid squares. The last three curves are shifted by factors of 10, 10^2, and 10^3 for clarity. Also shown are the data for the ten-times-diluted solution for the case $x = 1$ (diamonds). The dashed line shows the best linear fit (0.002–0.08 Å^{-1}) for the case $x = 0.5$, $q^{-1.4}$ decay, for comparison.

on literature data [38]:

$$CH_3\text{–}(CH_2)_9\text{–}CH_2\text{–}CH_2\text{–}O\text{–}CH_2\text{–}CH_2(O\text{–}CH_2CH_2)_4OH$$
$$a \quad b \quad c \quad d \quad g \quad e \quad f$$

There were no significant changes in the chemical shifts of the surfactant protons in the presence of the polymer, but changes were observed in the linewidth (given as the peak width at half-height, $\Delta\nu_{1/2}$), as can be seen in figure 3.

The peak due to the hydroxyl proton was not observed due to exchange with the solvent. A well resolved triplet was observed for the methyl group, which was unaffected by the presence of the polymer. However, changes were observed in the widths of the signals attributed to the methylene groups in the presence of polymer. These show up most clearly in the signal attributed to the protons c, which is unaffected by neighbouring groups on the surfactant chain. In the presence of ADS 181, an increase in the NMR linewidth of about 50% was observed with this signal, strongly suggesting a more restricted motion of the alkyl chain of the surfactant in the presence of the polymer due to some kind of polymer–surfactant complexation. This is in excellent agreement with the results of molecular dynamics simulations on the related PBS–PFP/$C_{12}E_5$ system (unpublished results), where the surfactant hydrocarbon chain is seen to bind close to the polymer backbone.

4. Small-angle neutron scattering

SANS was used to give an idea of the dissolution and self-organized structure formation of PFP-NR3 (and ADS 181) by the surfactant. While optical and NMR measurements probe very short ($\leqslant$nm) length scales, SANS brings information from between 3 and 300 nm. Figure 4 plots typical data for ADS 181 polymer in aqueous $C_{12}E_5$. Irrespective of the composition, all the curves are relatively similar and decay as -1.3–1.4 pointing to the structure of flexible cylinders. Even the data for the sample with the highest polymer fraction are close to those for pure amphiphile which intuitively indicates that polymer modifies the solution structure of aqueous $C_{12}E_5$ only a little. On the other hand the idea of worm-like cylinders is a natural idea for $C_{12}E_5$ as well as for semi-flexible π-conjugated polymers, so any other observation would be surprising. The data are also in agreement with those for the anionic conjugated polyelectrolyte PBS–PFP in the presence of the same surfactant [29]. At first sight the data for the sample diluted ten times are somewhat different, but essentially no concentration effect is seen.

Upon closer inspection of the data shown in figure 4 (shifted for clarity), it appears that the top four curves are virtually identical. All samples show the typical characteristics of the rod-like shape: nearly q^{-1} at lowest q and oscillation at high q (from which the radius could also be estimated), as well as an inflection point at about 0.008 Å^{-1}. To the left of it the decrease is steeper and to the right of it the slope is close to -1. This is an indication that both the local scales and the flexibilities are probed. The low q side would presumably change if the particle were to still substantially grow with increasing x, but this is not observed. The data for the denser (10 mM) samples could suggest the presence of more or less flexible aggregates which, however, consist of rigid cylindrical segments. From the inflection point ($\sim$0.01 Å^{-1}), we estimate the upper limit of the length of these segments to be $\sim$80 nm. The data for the dilute (1 mM) sample are somewhat different and show (with increasing q) the Guinier range of the cylinder and near -1 slope. At high q there may still be similar oscillation but this cannot be detected due to the weak signal. From this we can estimate the radius of gyration and the (upper limit of the) length of the rod to be $\sim$30 and $\sim$100 nm, respectively, for the particles in the dilute sample.

Interestingly, the dilute sample shows nearly monodisperse behaviour and this does not point to the existence of semi-flexible rods. When we consider the data for the denser (10 mM) samples, the growth processes and extra aggregation may take place. This, combined with the apparent similarity of the samples, makes more quantitative efforts at modelling the data for 10 mM samples difficult. On the other hand, the similarity of the curves implies that we are exploring mainly the local scale, but with just a small disturbance by longer length scales.

In view of the expected stiffness of the polymers, models with cylinder-like symmetry were selected. Although the semi-flexible chain model of Pedersen and Schurtenberger [39] probably provides the best intuitive approach for analysis, it did not yield physical parameters that could be understood well and therefore was rejected as a model fit function. The approach of the semi-flexible chain may not be better than simpler basic scattering forms. Instead, the randomly arranged core–shell cylinder model in a solvent with a minimum of parameters provided the experimentally observed dependence on q in terms of parameters. Here we use an absolute minimum of parameters which are controllable and which also describe

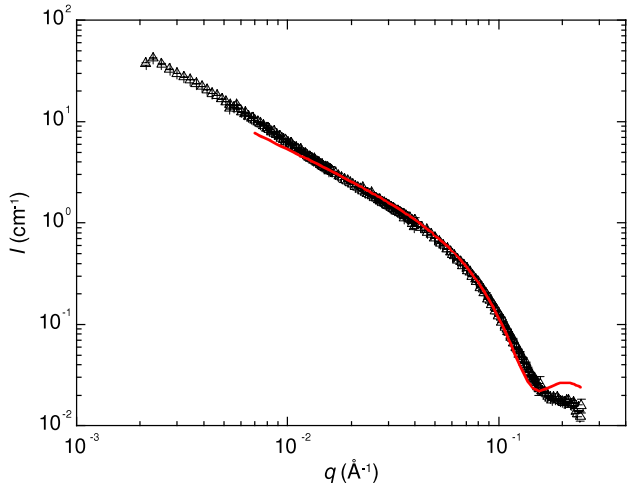

Figure 5. The SANS data for ADS 181$(C_{12}E_5)_x$ for $x = 0.5$ (triangles) as well as the model fitted to the data (red solid curve). The surfactant concentration was 10 mM in D_2O. See the text for details.

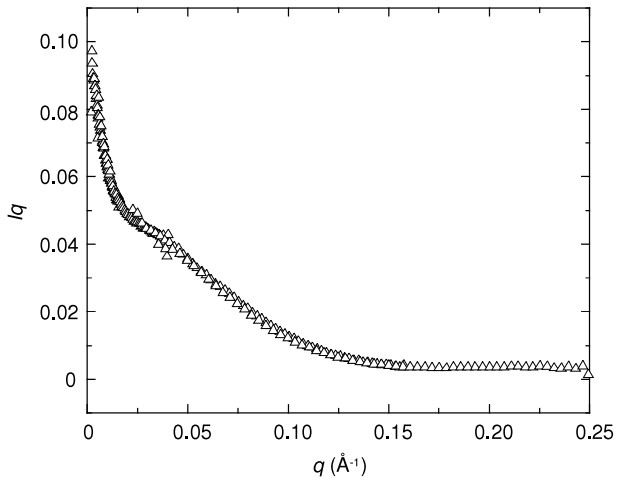

Figure 6. The Holtzer plot of the SANS data for ADS 181$(C_{12}E_5)_x$ for $x = 0.5$. The surfactant concentration was 10 mM in D_2O.

well the experimental dependence on q, only showing modest failings at the lowest scattering angles, although not on the length of cylinders. The difficulties at low angles may be due to aggregation or some polydispersity. A shell contribution is only taken into account in the form factor for cases where it is needed, but can be absorbed easily in either of the two components.

In detail, the model that we propose is produced as follows. Firstly, the neutron scattering intensity which is the probability of scattering into a solid angle dΩ, normalized to the scattering volume, is given generally as

$$\frac{\mathrm{d}\Sigma}{\mathrm{d}\Omega}(q) = N(\Delta\rho)^2 V^2 P(q) = \phi(\Delta\rho)^2 V P(q), \qquad (2)$$

where N is the number density, V the scattering particle volume and ϕ its volume fraction. $P(q)$ is the form factor of the core–shell cylindrical particle to be adjusted to the data. Then, the random orientation of the cylinder over the angle α that the cylinder makes with the q-axis will be taken into account by averaging the scattering amplitude through

$$P(q) \sim \int_0^{\pi/2} F^2(q, \alpha) \sin\alpha \, \mathrm{d}\alpha. \qquad (3)$$

For this three-component system in two phases, the scattering will then be calculated using

$$\begin{aligned} F(q,\alpha) &= 2(\rho_{\mathrm{core}} - \rho_{\mathrm{shell}}) V_{\mathrm{core}} j_0(qL\cos\alpha/2) \\ &\quad \times J_1(qR\sin\alpha)/(qR\sin\alpha) \\ &\quad + 2(\rho_{\mathrm{shell}} - \rho_{\mathrm{solvent}}) V_{\mathrm{tot}} j_0(q(L+t)\cos\alpha/2) \\ &\quad \times J_1(q(R+t)\sin\alpha)/(q(R+t)\sin\alpha) \end{aligned} \qquad (4)$$

where $j_0(x) = \sin x/x$, R is the radius, t the thickness of the layer and L the full length, and J_1 is the first-order Bessel function. The model assumes both ends of the cylinder to be covered as well. Finally the integration is done numerically and the best fit result for ADS 181$(C_{12}E_5)_{0.5}$ is shown in figure 5. Figure 6 shows the Holtzer plot of the same data for comparison. We stress that here we can use the form factor over the full range of q to obtain L and R. For comparison, they can also be estimated from the inflection points and the position of the minimum at high q.

On the basis of consideration above we find that the length of the cylindrical ADS 181$(C_{12}E_5)_{0.5}$ in water is of the order of 60 nm and the radius is approximately 2.5 nm. The thickness of the shell was a parameter which was included to improve the fit quality if needed but could be fixed to quasi-zero by either fixing its size to 0 or equalizing its contrast to the solvent. As the data were calibrated absolutely, scattering contrasts as calculated could be inserted and the k_{pet} constant set to its theoretical value. The q^{-1} behaviour, evident in the first term in front of the Bessel function produces a q-independent line and provides easy graphical proof of the presence of the cylinder if the data are shown in the first moment of the intensity. The same can, however, be seen from normal log–log plots (figure 4). In contrast, the separation into longitudinal and cross-sectional parameters as often proposed for thin cylinders does not have to be a correct description. We have therefore not attempted to decouple. Some model-independent information can be obtained in addition to this decoupling. From consideration of the structure factor, it can be seen that the first minimum in the oscillation delivers direct information about the size of the radius of the object. For a cylinder the term $(J_1(x)/x)^2$ ($x = qR$) shows its first minimum at $x \sim 3.83$ approximately from which a starting parameter for a full fit can be extracted. For the case of a sphere this minimum would shift to an x value of about 4.49. Finally from the data for ADS 181$(C_{12}E_5)_{0.5}$ (shown in figure 5) a radius of about 2.8 nm can be determined, in excellent agreement with the full fit. Hence, the cylindrical segment of the length of 60 nm and the radius of 2.8 nm is expected to represent a fairly accurate structural picture of ADS 181 polymer in aqueous $C_{12}E_5$ surfactant solutions.

As seen in figure 4, all ADS 181 samples are relatively similar regardless of the molar ratio or concentration and,

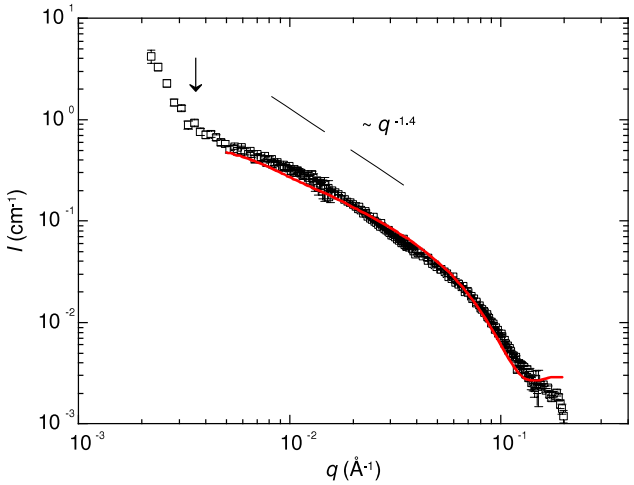

Figure 7. The SANS data for PFP-NR3 $(C_{12}E_5)_x$ for $x \approx 1$ (open squares) as well as the model fitted to the data (red solid curve). See the text for details. A dashed line shows the best linear fit (0.002–0.08 $Å^{-1}$), $q^{-1.4}$ decay, for comparison.

therefore, in order to better understand this system attention was focused on another related polymer, PFP-NR3 (figure 1). This polymer is similar to ADS 181, but its molecular weight is slightly less than half of that of ADS 181, so it can be considered to be a π-conjugated oligomer. In figure 7, typical data are plotted for an aqueous PFP-NR3($C_{12}E_5$) sample treated similarly to those samples with ADS 181, as well a model curve fitted to the data, the model being based on the concepts described above. The data depicted in figure 7 are reminiscent of those shown in figure 5, pointing to worm-like particles. Nevertheless, there is a distinctive upturn at around 0.004 $Å^{-1}$ (marked by an arrow). Moreover, compared to the ADS 181 data, the inflection point is at higher q ($\sim$0.015 $Å^{-1}$). This means that the cylindrical objects are shorter than in the case of ADS 181 and from the plot we estimate persistent segments to be 40 nm long. From the fit we estimate a value of 50 nm. In this picture these segments are then part of the far longer worm-like chain. From this, a diameter of 2.5 nm is obtained, which is fairly similar to the value calculated for the ADS 181($C_{12}E_5$). We may also interpret the lower q data as the Guinier region for the cylinder, which would give us 12.5 nm for the radius of gyration and more or less 45 nm for the length of the cylinder.

The finding of shorter objects is intuitively reasonable considering the difference in backbone length of the polymers (molecular weight). Equally, it is plausible that the diameters are similar, as the molecular weight probably does not influence the local ordering. In addition, as pointed out by a referee, it is possible that, as with polyfluorenes [40], the backbone has a helicoidal form. This would be expected to favour the observed interactions of these cationic conjugated polyelectrolytes with nucleic acids [8, 13, 15]. We finally note that the solubility characteristics of these polymers are not identical and no cloudiness or precipitation was observed for ADS 181, whereas some non-dissolved particles were observed for PFP-NR3 with relatively long measurement time. Therefore, the latter data should be interpreted with care.

5. Conclusions

In conclusion, two cationic fluorene based conjugated polymers with different molecular weights in aqueous solution in the presence of the surfactant $C_{12}E_5$ have been studied using optical absorption and fluorescence, NMR, and SANS with a model of randomly arranged core–shell cylinders in a solvent. All the results show that the surfactant solubilizes the polymer by formation of some mixed polymer–surfactant species. SANS data suggest that upon dissolution, these $C_{12}E_5$/polymer systems form long worm-like particles which contain rigid segments with the diameter of 2.5 nm. The polymers studied differ from each other in the respect that the ternary system with ADS 181 has longer rigid segments than the one with PFP-NR3. For the former one we calculate a typical value of more than 60 nm and for the latter one a typical value of 45 nm. This difference is rationalized in terms of the difference in polymer length. Future experiments are planned using cryo-transmission electron microscopy to visualize the structures formed.

Acknowledgments

This research project was supported by the European Commission under the 6th Framework Programme through the Key Action: Strengthening the European Research Area, Research Infrastructures. Contract No RII3-CT-2003-505925. Financial support from POCI/FCT/FEDER through the project POCI/QUI/58291/2004, and from MEC and FEDER through the project MAT2004-03827 is gratefully acknowledged. SMF thanks the FCT for the award of a postdoctoral fellowship.

References

[1] Chen L, McBranch D W, Wang H-L, Helgeson R, Wudl F and Whitten D G 1999 *Proc. Natl Acad. Sci.* **96** 12287
[2] Wang D, Gong X, Heeger P S, Rininsland F, Bazan G C and Heeger A J 2002 *Proc. Natl Acad. Sci* **99** 49
[3] Gaylord B S, Heeger A J and Bazan G C 2002 *Proc. Natl Acad. Sci.* **99** 10954
[4] Fan C, Plaxco K W and Heeger A J 2005 *Trends Biotechnol.* **23** 186
[5] Wang S and Bazan G C 2004 *Chem. Commun.* 2508
[6] Mallavia R, Martinez-Peréz D, Chmelka B F and Bazan G C 2004 *Bol. Soc. Esp. Ceram. V.* **43** 327
[7] Liu B and Bazan G C 2006 *J. Am. Chem. Soc.* **128** 1188
[8] Liu B and Bazan G C 2004 *Chem. Mater.* **16** 4467
[9] Pinto M R and Schanze K S 2003 *Synthesis-Stuttgart* **9** 1293
[10] DiCesare N, Pinto M R, Schanze K S and Lakowicz J R 2002 *Langmuir* **18** 7785
[11] Pinto M R and Schanze K S 2004 *Proc. Natl Acad. Sci.* **101** 7505
[12] Lavigne J J, Broughton D L, Wilson J N, Erdogan B and Bunz U H F 2003 *Macromolecules* **36** 7409
[13] Taira S and Yokoyama K 2004 *Biotech. Bioeng.* **88** 35
[14] Thomas S W, Joly G D and Swager T W 2007 *Chem. Rev.* **107** 1339
[15] Al Attar H A and Monkman A P 2007 *J. Phys. Chem.* B **111** 12418
[16] Xia C, Locklin J, Youk J H, Fulghum T and Advincula R C 2002 *Langmuir* **18** 955
[17] Huang F, Hou L, Wu H, Wang X, Shen H, Cao W, Yang W and Cao Y 2004 *J. Am. Chem. Soc.* **126** 9845

[18] Ma W, Iyer P K, Gong X, Liu B, Moses D, Bazan G C and Heeger A J 2005 *Adv. Mater.* **17** 274
[19] Wilson J S, Frampton M J, Michels J J, Sardone L, Marletta G, Friend R H, Samori P, Anderson H L and Cacialli F 2005 *Adv. Mater.* **17** 2659
[20] Dang T D, Bai S J, Heberer D P, Arnold F E and Spry R J 1993 *J. Polym. Sci.* B **31** 1941
[21] Decher G 1997 *Science* **277** 1232
[22] Baur J, Rubner M F, Reynolds J R and Kim S 1999 *Langmuir* **15** 6460
[23] Kawase T, Shimoda T, Newsome C, Sirringhaus H and Friend R H 2003 *Thin Solid Films* **438/439** 279
[24] Schubert U 2005 *Macromol. Rapid Commun.* **26** 237
[25] Scherf U and List E J W 2002 *Adv. Mater.* **14** 477
[26] Rulkens R, Wegner G and Thurn-Albrecht T 1999 *Langmuir* **15** 4022
[27] Burrows H D, Lobo V M M, Pina J, Ramos M L, Seixas de Melo J, Valente A J M, Tapia M J, Pradhan S and Scherf U 2004 *Macromolecules* **37** 7425
[28] Burrows H D, LoboV M M, Pina J, Ramos M L, Seixas de Melo J, Valente A J M, Tapia M J, Pradhan S, Scherf U, Hintschich S I, Rothe C and Monkman A P 2005 *Colloids Surf.* A **270/271** 61
[29] Knaapila M, Almásy L, Garamus V M, Pearson C, Pradhan S, Petty M C, Scherf U, Burrows H D and Monkman A P 2006 *J. Phys. Chem.* B **110** 10248
[30] Tapia M J, Burrows H D, Knaapila M, Monkman A P, Arroyo A, Pradhan S, Scherf U, Pinazo A, Pérez L and Morán C 2006 *Langmuir* **22** 10170
[31] Burrows H D, Tapia M J, Silva C L, Pais A A C C, Fonseca S M, Pina J, Seixas de Melo J, Wang Y, Marques E F, Knaapila M, Monkman A P, Garamus V M, Pradhan S and Scherf U 2007 *J. Phys. Chem.* B **111** 4401
[32] Fütterer T, Hellweg T, Findenegg G H, Frahn J, Schlüter A D and Böttcher C 2003 *Langmuir* **19** 6537
[33] Knaapila M, Stepanyan R, Lyons B P, Torkkeli M and Monkman A P 2006 *Adv. Funct. Mater.* **16** 599
[34] Stork M, Gaylord B S, Heeger A J and Bazan G C 2002 *Adv. Mater.* **14** 361
[35] Becker R S, Seixas de Melo J, Maçanita A L and Elisei F 1996 *J. Phys. Chem.* **100** 18683
[36] Miller J N (ed) 1981 *Standards in Fluorescence Spectrometry* (London: Chapman and Hall)
[37] Carless M J E, Challis R and Mulley B 1964 *J. Colloid Interface Sci.* **19** 201
[38] Christenson H and Friberg S 1980 *J. Colloid Interface Sci.* **75** 276
[39] Pedersen J S and Schurtenberger P 1996 *Macromolecules* **29** 7602
[40] Knaapila M, Torkkeli M and Monkman A P 2007 *Macromolecules* **40** 3610